

# Optimal and thermal design in transitional condition of a paraboloidal solar furnace for the hydrogen production

Fermin Aguilar<sup>1</sup>, J. Luis Contreras L<sup>1</sup>, Beatriz Cruz-Munoz<sup>2</sup> and Ruben Dorantes-Rodriguez<sup>1</sup>

<sup>1</sup> Universidad Autónoma Metropolitana, Azcapotzalco.

Av. San Pablo 180, Col. Reynosa Tamaulipas. CP02200 Mexico City, Mexico

<sup>2</sup> Universidad Tecnológica de Pereira, Colombia

Carrera 27 No. 10-02. Los Alamos. CP. 660003 Pereira, Colombia

## Abstract

We present the results of the optical and thermal simulation in temporary state of a parabolic solar concentrator combined with a chemical reactor to produce hydrogen. In a previous experimental work, the reaction of ethanol steam reforming (ESR) based on a bimetallic catalyst Ni-Co-Hidrotalcita-WO<sub>x</sub> (HTB-3) with high selectivity for H<sub>2</sub>, was tested. The activation temperature of the catalyst was 450 °C and this temperature was maintained for 30 min more to make three chromatographic analyzes. This process was carried out at three temperatures (450 °C, 500 °C and 550 °C). To replace the electrical power necessary for the reaction (1200 W) a paraboloidal solar concentrator was designed. Geometric parameters of the paraboloid were calculated, such as the area, angle of opening and the focus, determining the most convenient geometry to concentrate the solar power required. A temporary energy balance was made in the solar concentrator to calculate the heat needed for the chemical reactor. We solved the differential equation by finite differences to calculate the reactor temperature and keep it stable as long as possible. The results show that the solar concentrator operating in Hermosillo Sonora, with an irradiance greater than 900 W/m<sup>2</sup>, reaches average temperatures above 700 °C in 15 minutes and remains stable for more than 7 hours, showing the technical viability of the equipment. It is demonstrated that it is feasible to carry out the ethanol vapor reforming reaction using conditions similar to those carried out when the reactor was heated with an electric oven. The reaction products were mainly H<sub>2</sub>, CH<sub>4</sub> and CO<sub>2</sub>.

*Keywords: Paraboloidal, solar furnace, chemical, reactor, hydrogen*

---

## 1. Introduction

Large-scale production of biofuels offers a development opportunity for developing countries and thus reduce their dependence on oil. For this reason, biomass-derived fuels such as bioethanol, biodiesel and hydrogen play an important role today and in the near future of the world and from here using traditional thermochemical or biological processes to obtain hydrogen [2]. Hydrogen production is one of the most promising alternative energy technologies, however it is not a primary resource freely available in nature. Most experts believe that hydrogen will have a great role to play as an energy carrier in the global energy sector [3,4], for several reasons: it is a clean fuel, without CO<sub>2</sub> emissions and can easily be used in fuel cells of electric vehicles, as well as in the generation of domestic electricity. In addition, hydrogen has a high energy efficiency (122 KJ/g), which makes it more attractive for use in combustion engines. For transport and various applications it is receiving much more favorable attention as a technical and vision issue in public policy [5].

Global hydrogen production in 2008 reached 13 billion standard cubic feet [6] and on the order of 10% of that amount was supplied by industrial companies; the rest was produced by consumers themselves within their chemical plants to meet their demand, such as refineries and ammonia and methanol production facilities. A logical source for large-scale hydrogen production is water, which is an abundant molecule in the earth. Different methods of producing hydrogen from water have been or are being developed [7]. These include studies based on Electrolysis, Thermochemical Processes, Photolysis, Photoelectrochemical Processes and Photocatalysis Biomass is another important renewable resource used for the production of hydrogen [7]. The main disadvantages of these processes, which make them unfeasible in the long term for the production of hydrogen is the generation of important greenhouse gas emissions, such as CO<sub>2</sub> and by depleting fossil resources. Solar energy, as a renewable source and for its extraordinary abundance, is a viable option to mitigate both inconveniences. Solar energy can be concentrated to obtain the high temperatures required for efficient solar thermochemical processes. When solar radiation is used

as an energy source to produce energy, such as synthesis gas (which is a mixture of H<sub>2</sub> and CO, they are called “solar fuels” (HI Villafán-Vidales) [7]. These processes are also an alternative route to the storage of solar energy in chemical form, helping to compensate for the intermittency of the solar resource, so “solar fuels” such as hydrogen production where the energy consumed is of solar-thermal origin, can be used in different ways: improving fossil fuels that are burned to generate heat, using them directly in burners, in turbines or engines to produce electricity or movement, or using them to generate electricity in fuel cells and batteries. The methods for producing hydrogen with solar energy are grouped into three large sets [7]: photochemical, electrochemical and thermochemical processes, although there are also combinations of the above (photoelectrolysis, high temperature electrolysis of steam).

This study will focus on methods that use concentrated solar energy and thermochemical methods, including: direct water thermolysis, thermochemical cycles, usually two-step, based on the reduction of metal oxides, as well as cracking, reformed and gasification of hydrocarbons. To achieve high concentration ratios, one of the three most common optical configurations is used: parabolic discs and torrencentral systems and cylindrical-parabolic collectors, although the necessary temperature level is not reached with the latter.

## 2. Previous studies

In 2015, A. Jaramillo and N. Daza [8], carried out the design and experimental study of a solar stove shaped like a paraboloid of revolution, based on the methodology presented by P F Diez [1]. In addition, an optical model of the paraboloid was coupled with a thermal model of the receiver located at the focal point of the paraboloid, to reach the desired temperature. Experimentally and using thermal oil as a working fluid in the receiver, a temperature of 180 °C was reached in a short time. In 2016, L. A. Andrade et al. [9] presented a paper where they predict the behavior of temporal temperature in a specimen placed at the focal point of a parabolic solar concentrator, where a  $\Omega$  dimension is proposed, which correlates the diameter of the solar collector (D) with the solid mass at heat (M) and solar irradiance (I). The authors also investigated the equilibrium temperature behavior as a function of  $\Omega$ . The simulations were carried out by manipulating D, M and G, and organized according to a complete factorial design. The simulation results obtained showed that temperatures of up to 1600 °C can be reached in relatively short periods of time, and may be an alternative to obtain energy of high temperature.

In 2016, I. Martínez [10] carried out the experimental study of a catalytic bed reactor for the production of hydrogen from bioethanol and using electrical resistors as a source of heat. It resulted in the evaluation of the catalyst at three different temperatures (450 °C, 500 °C and 550 °C).

In 2017, H.I. Villafán-Vidales et al. [7] present an overview of solar thermochemical processes for the production of hydrogen and synthesis gas. They indicate that biomass gasification is a complex process that involves several reactions that require high temperatures. According to their study, gasification represents a capacity of 430 Mm<sup>3</sup> of the world's daily production of hydrogen [5]. Thus, the use of solar energy concentration in the gasification process has several advantages: (a) almost 30% of CO<sub>2</sub> emissions can be reduced, (b) 5%–25% of the raw material can be saved and (c) higher yields of synthesis gas per unit of biomass can be obtained, since it eliminates the need to consume part of the biomass as fuel to provide heat to the process.

Several prototypes of solar reactors have been developed. One of the first solar prototypes was proposed in the 1980s and was a directly irradiated compact bed [11], using reagents such as sub-bituminous coal, activated carbon, coke and a mixture of coal and biomass with steam and CO<sub>2</sub> as gasifying agents. The reactor consisted of an L-shaped stainless steel cavity. This reactor was tested in White Sands, New Mexico. With this prototype, the authors achieved energy conversions with efficiencies between 4.8% and 8.6% and average molar flows of 0.2 mol/min of H<sub>2</sub>, 0.064 mol min of CO, 0.04 mol/min of CO<sub>2</sub>, and 0.007 mol/min of CH<sub>4</sub>, with a synthesis quality of H<sub>2</sub>: CO  $\approx$  3 which, according to the authors, is superior to that obtained in a conventional gasification process.

## 3. Design of a solar concentration system

### 3.1 Classification of solar concentrators.

There are four technologies to obtain Solar Thermal Concentration Energy: Fresnel Linear Concentrator Systems (LFR), Central Receiver Systems or Solar Tower, Parabolic Disk Systems and Parabolic Channels. As the geometry of the chemical reactor is cylindrical, parabolic disk technology was chosen.

### 3.1.1 Parabolic disk systems.

A disk-shaped parabolic reflector concentrates the sun's rays into a receiver located at the focal point of the disk. The concentrated radiation is absorbed into the receiver to heat a fluid or gas (air) to about 750 °C, for example, as a high-temperature heat-carrier fluid for a reaction (Fig. 1).

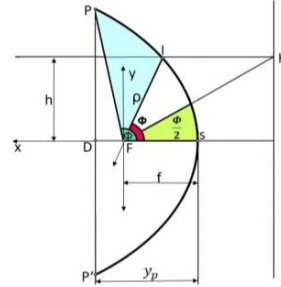
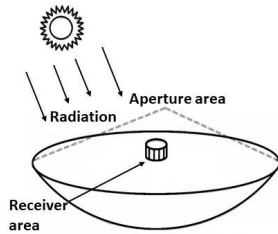


Fig. 1: Opening area and area of the paraboloid receiver [1]. Fig. 2: Geometry of a parabola in polar coordinates [1].

### 3.1.2 Concentration factor

The concentration factor  $C$  of the area is given as the relationship between the opening area ( $A_a$ ) and the area of the receiver ( $A_r$ ) (Fig. 1 and Fig. 2) [1].

$$C = A_a / A_r \quad (\text{Eq. 1})$$

### 3.1.3 Design of a parabolic solar concentrator revolution.

To calculate the area of the paraboloid in revolution (resulting from the rotation of a parabola around its axis), it is necessary to know the equation that describes the geometric figure [1].

$$x^2 = 4py \quad (\text{Eq. 2})$$

Where,  $p$  is a focal point of the parabola. To know the equation of the parabola in spherical coordinates, the concept of eccentricity is used, which although for conical function is one, establishes the relationship between a point of the function and the focus, and a fixed line and that is given by .

$$\tau = \frac{\overline{IF}}{\overline{IH}} = \frac{\rho}{2f - \rho \cos \phi} \quad (\text{Eq. 3})$$

Where,  $\rho$  is the distance between the focal point (F) and any point of the parabola (I),  $f$  is the focal length,  $\phi$  is the opening angle of  $\rho$ , H is a point of the direct line, S is the vertex of the parabola, P is the end point of the parabola, D is the distance between the end points and  $h$  is the height of the point I (Fig. 2).

So the equation that describes the parabola in polar coordinates is:

$$\rho = \frac{2f}{1 + \cos \phi} = \frac{f}{\cos^2 \frac{\phi}{2}} \quad (\text{Eq. 4})$$

The relation for the angle is also obtained  $\phi$  [8]

$$\tan \frac{\phi}{2} = \frac{h}{2f} \quad (\text{Eq. 5})$$

Considering the maximum opening angle ( $\phi_{\max} = \phi$ ), the diameter of the entire parabola is  $D = 2h$ , so that in terms of the focal length is: [1]

$$D = 4f \tan \frac{\phi}{2} \quad (\text{Eq. 6})$$

The opening area of the paraboloid is the surface that is formed with the largest diameter of the parabola, is circular in shape and is found from the following equation.

$$Aa = \frac{\pi}{4} D^2 \quad (\text{Eq. 7})$$

Replacing the diameter in the previous equation, the opening area must finally be:

$$Aa = 4\pi f^2 \tan^2 \frac{\phi}{2} \quad (\text{Eq. 8})$$

However, it is necessary to know the area of the paraboloid in revolution, which is from the first Pappus-Guldin theorem (Fig. 3), where it is established, that if there is a curve of length L and it is rotated around an axis, an area revolution is generated  $A_\phi$  to find this area it is enough to multiply the distance traveled by the centroid of the curve (C), by the length of itself.

$$A_\phi = \int_0^\phi 2\pi \bar{y} dl \quad (\text{Eq. 9})$$

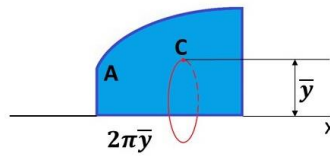


Fig. 3: First theorem of Pappus Guldin [1].

In the case of the paraboloid in revolution the coordinate  $\bar{y}$  is equal to:

$$\bar{y} = \rho \sin \phi \quad (\text{Eq. 10})$$

Replacing the value of  $\rho$  previously obtained we obtain:

$$\bar{y} = \frac{f \sin \frac{\phi}{2}}{\cos^2 \frac{\phi}{2}} \quad (\text{Eq. 11})$$

For the calculation of the length differential, the parabola equation (eq. 2) is derived:

$$d\rho = \frac{\left(-2f \cos \frac{\phi}{2}\right) \left(-\sin \frac{\phi}{2}\right)}{\cos^4 \frac{\phi}{2}} \frac{d\phi}{2} \quad (\text{Eq. 12})$$

Simplifying the previous equation,

$$d\rho = \frac{f \sin \frac{\phi}{2}}{\cos^3 \frac{\phi}{2}} d\phi \quad (\text{Eq. 13})$$

Replacing Eq. 13 in the length differential for polar coordinates:

$$dl^2 = d\rho^2 + (\rho d\phi)^2 \quad (\text{Eq. 14})$$

$$dl^2 = \left(\frac{f \sin \frac{\phi}{2}}{\cos^3 \frac{\phi}{2}} d\phi\right)^2 + \left(\frac{f}{\cos^2 \frac{\phi}{2}} d\phi\right)^2 \quad (\text{Eq. 15})$$

Factoring the previous expression we have:

$$dl^2 = \frac{f^2 d\phi^2}{\cos^4 \frac{\phi}{2}} \left( \frac{\sin^2 \frac{\phi}{2}}{\cos^2 \frac{\phi}{2}} + 1 \right) \quad (\text{Eq. 16})$$

Applying the trigonometric identity:

$$\sin^2 \theta + \cos^2 \theta = 1 \quad (\text{Eq. 17})$$

$$dl^2 = \frac{f^2 d\phi^2}{\cos^4 \frac{\phi}{2}} \left( \frac{1}{\cos^2 \frac{\phi}{2}} \right) \quad (\text{Eq. 18})$$

Reorganizing the previous equation and taking square root on both sides, you have that the length differential ( $dl$ ) of the curve that describes the parabola is:

$$dl = \frac{f d\phi}{\cos^3 \frac{\phi}{2}} \quad (\text{Eq. 19})$$

Taking the equation of the area of the parabola (Eq. 9) and replacing the expressions found above (Eq. 11 and Eq. 19) you get:

$$A_\phi = 2\pi \int_0^\phi \frac{f^2 \sin \frac{\phi}{2}}{\cos^5 \frac{\phi}{2}} d\phi \quad (\text{Eq. 20})$$

Using the trigonometric identity of sum of angles:

$$\sin(\phi) = 2 \sin \frac{\phi}{2} \cos \frac{\phi}{2} \quad (\text{Eq. 21})$$

Replacing Eq. 21 in Eq. 20:

$$A_\phi = 4\pi f^2 \int_0^\phi \frac{\sin \frac{\phi}{2}}{\cos^4 \frac{\phi}{2}} d\phi \quad (\text{Eq. 22})$$

Using the method of integration by parts and separating the integral, where:

$$u = \frac{1}{\cos^4 \frac{\phi}{2}} \quad ; \quad dv = \sin \frac{\phi}{2} d\phi \quad ; \quad du = \frac{2 \sin \frac{\phi}{2}}{\cos^5 \frac{\phi}{2}} d\phi \quad ; \quad v = -2 \cos \frac{\phi}{2} d\phi$$

$$\text{and} \quad \int_0^\phi \frac{\sin \frac{\phi}{2}}{\cos^4 \frac{\phi}{2}} d\phi = -\frac{2}{\cos^3 \frac{\phi}{2}} + 4 \int_0^\phi \frac{\sin \frac{\phi}{2}}{\cos^4 \frac{\phi}{2}} d\phi \quad (\text{Eq. 23})$$

Adding the integrals of both sides

$$4 \int_0^\phi \frac{\sin \frac{\phi}{2}}{\cos^4 \frac{\phi}{2}} d\phi - \int_0^\phi \frac{\sin \frac{\phi}{2}}{\cos^4 \frac{\phi}{2}} d\phi = \frac{2}{\cos^3 \frac{\phi}{2}} \quad (\text{Eq. 24})$$

So the integral obtained is:

$$\int_0^\phi \frac{\sin \frac{\phi}{2}}{\cos^4 \frac{\phi}{2}} d\phi = \frac{2}{3 \cos^3 \frac{\phi}{2}} \quad (\text{Eq. 25})$$

Replacing equation 17 in Eq. 22, we get:

$$A_\phi = 4\pi f^2 \left. \frac{2}{3 \cos^3 \frac{\phi}{2}} \right|_0^\phi \quad (\text{Eq. 26})$$

Finally, the area of the parabola after evaluating the previous equation is:

$$A_{\phi} = \frac{8\pi f^2}{3} \left( \frac{1}{\cos^3 \frac{\phi}{2}} - 1 \right) \quad (\text{Eq. 27})$$

At the beginning of the Eq. 27 the area of the parabola can be calculated when determining the focus  $f$  and the opening angle  $\phi$ , which will be selected in order to determine a parabola, to design a concentrator that concentrates the power necessary to reach the reactor operating temperature.

### 3.1.4 Paraboloid area, height and focus.

To calculate the height of the parabola, it is necessary to resort again to Fig. 2, which results in the following relationship: [1,8]

$$y_p = f + \rho \cos(180 - \phi) \quad (\text{Eq. 28})$$

Using the following trigonometric identity:

$$\cos(a - b) = \cos a \cos b + \sin a \sin b \quad (\text{Eq. 29})$$

It has for  $y_p$ :

$$y_p = f - \rho \cos(\phi) \quad (\text{Eq. 30})$$

Replacing Eq. 4 in Eq. 30, we get:

$$y_p = f \left( 1 - \frac{\cos \phi}{\cos^2 \frac{\phi}{2}} \right) \quad (\text{Eq. 31})$$

Then the equations corresponding to the geometric and optical design of the paraboloid, its focus and its height have been established. The resulting values of these equations will be used as parameters of each simulation and thus solve the mathematical model that determines the concentration necessary to reach the starting temperature for the chemical reaction that will produce hydrogen.

## 4. Energy balance using a catalytic reactor as an absorber

To evaluate the thermal performance of the paraboloidal concentrator (Fig. 4), the catalytic bed reactor was considered as the absorber placed at the focal point, and using a temporary energy balance, (Fig. 5) where it is established that

the difference of the sum of the input energy flows ( $\dot{Q}_{in}$ ) minus the sum of the output flows

( $\dot{Q}_{out}$ ), is practically equal to the temporary change of the internal energy of the  $dE / dt$  system, that is:

$$\sum \dot{Q}_{in} - \sum \dot{Q}_{out} = \frac{dE}{dt} \quad (\text{Eq. 32})$$

that written in another way, (Eq.32) becomes:

$$\sum \dot{Q}_{in} - \sum \dot{Q}_{out} = (m_{mezc} c_{mezc} + m_{reac} c_{reac}) \frac{dT}{dt} \quad (\text{Eq.33})$$

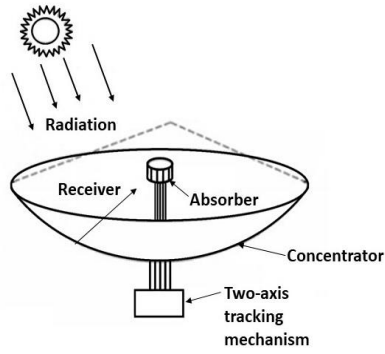


Fig. 4: Parabolic Disc Concentration Collector. [1]

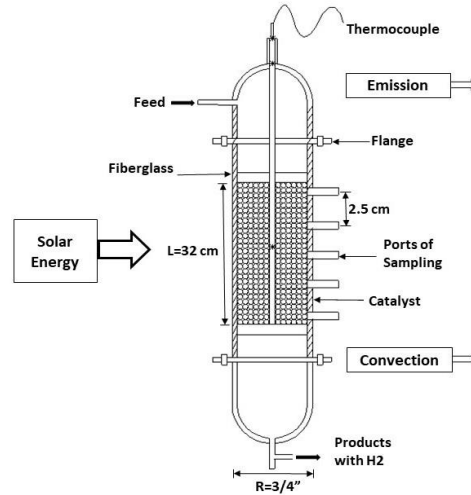


Fig. 5: Energy balance. [11]

where  $m_{mezc}$  and  $c_{mezc}$  are the specific mass and heat of the reactor, while  $m_{reac}$  and  $c_{reac}$  are the specific mass and heat of the components of the reaction to be heated,  $dT$  is the temperature differential of the reactor and  $dt$  is the time differential. Solving the (Eq. 33) by finite differences, where from a starting temperature  $T_j$ , a value of it is calculated after an instant of time  $\Delta t$ ,  $T_{j+1}$ , which allows to theoretically estimate the temporal evolution of the temperature that the reactor would reach, such that:

$$\frac{dT}{dt} = \frac{T_{(j+i)} - T_j}{\Delta t} \quad (\text{Eq. 34})$$

Replaced in Eq.33 the Eq.34 and reorganizing, the Eq.35 is obtained, which allows to calculate the increase of the initial temperature of the system  $T_j$  after a time  $\Delta t$ , until reaching the final temperature  $T_{j+1}$ , which it will depend fundamentally on the optical behavior of the paraboloidal concentrator with the absorber (gains and losses of heat and increase of the internal energy) and of the solar radiation of the moment (Eq. 35).

$$T_{(j+1)} = T_j + \frac{\Delta t}{(m_{mezc}c_{mezc} + m_{reac}c_{reac})} \left( \sum \dot{Q}_{in} - \sum \dot{Q}_{out} \right) \quad (\text{Eq. 35})$$

#### 4.1.1 Energy gains in a thermochemical solar heating process.

The input power in a parabolic solar concentrator to heat the reactor in a certain time, is expressed as:

$$Q_{rad} = \alpha R I A_p \quad (\text{Eq. 36})$$

Where  $\alpha$  is the absorption coefficient of the reactor (metal + absorbent film),  $R$  the reflection coefficient of the film that covers the surface of the parabolic disk of revolution,  $I$  the solar irradiation and  $A_p$  the surface area of the concentrator.

#### 4.1.2 Loss of energy

In a thermochemical process of convection heating, emission, conduction, and reaction energy. The most common way to reduce heat loss in the receiver at elevated temperatures is to reduce its size, since heat loss is directly proportional to its area.

##### 4.1.2.1. Convection.

Convection losses is one of the factors that most influence the performance of the device [8], which is a function of the convection heat transfer coefficient of the material  $h_{ca}$ ,  $T_e$  and  $T_0$  the temperature of the absorber and the ambient air and  $A_{reac}$  is the surface area of the reactor, such that:

$$\sum \dot{Q}_{conv} = A_{reac} h_{ca} (T_e - T_o) \quad (\text{Eq. 37})$$

The convection coefficient  $h_{ca}$  (Eq. 38) also depends on the speed and incidence of the place's wind, and is influenced by the surface finish of the absorber. For this work, an air current perpendicular to the receiving surface was considered, where  $v_{aire}$  is the average wind speed (in m/s), such that:

$$h_{ca} = 16.9v_{aire}^{0.45} \quad (\text{Eq. 38})$$

#### 4.1.2.2 Emission.

These losses can be determined from the Stefan Boltzman equation, such that:

$$\sum \dot{Q}_{emi} = A_{react} \sigma \xi (T_e^4 - T_0^4) \quad (\text{Eq. 39})$$

Where  $A_{react}$  is the surface area of the reactor,  $\sigma$  is the constant of Stefan Boltzman ( $5.67 \times 10^{-8} \text{ W/m}^2\text{K}^4$ ),  $\xi$  is the emissivity coefficient of the absorber material,  $T_e$  the average temperature of the absorber and  $T_0$  the temperature of the medium.

#### 4.1.2.3 Conduction

In the case of the absorber, the conduction heat losses are negligible because the contact area between the reactor and the clamping structure is minimal, so these will not be taken into account, since the exposed area is directly proportional to driving losses, as shown in Eq. 40. [8]

$$\sum \dot{Q}_{cond} = \frac{\lambda A_{react} (T_e - T_{est})}{d} \quad (\text{Eq. 40})$$

Where  $\lambda$  is the thermal conductivity of the absorber,  $A_{react}$  the contact area,  $T_e$  the temperature of the absorber,  $T_{est}$  the temperature of the structure and  $d$  its thickness [8].

#### 4.1.2.4 Reaction Energy

Reaction energy is the energy needed to activate the reaction and start producing hydrogen. Experimentally, a pair of electrical resistors of 600W each was used [10], therefore in the simulation of the parabolic concentrator this reaction energy was considered.

$$Q_{reaction} = 1200 \text{ W} \quad (\text{Eq. 41})$$

### 4.2 Algorithm of resolution of the mathematical model, initial conditions used and results.

To solve the mathematical model developed above, an Excel sheet was used, with the algorithm presented in (Fig. 6) and using the meteorological data of solar irradiation, ambient temperature and wind speed, provided every 10 minutes by the Meteorological Stations from four Mexican cities.

## 5. Results and Discussion

### 5.1. Thermal behavior

For the analysis of the thermal behavior of the absorber (reactor), data from some days of June and July 2018, of four Mexican cities, two of moderate climate and two of extreme climate, but all with very irradiation conditions were used. It was possible to characterize a reactor temperature profile against time, simulating the behavior of the parabolic concentrator from 9 am to 6 pm, evaluated every hour in the cities of: Hermosillo Sonora, Mexico City (CDMX), Cuernavaca Morelos and Morelia Michoacán.

In Fig. 7 the different reactor temperature profiles for the different cities are observed, where a reference temperature band between 600 °C and 800 °C has been used. For the city of Hermosillo (blue color), a profile of increasing, stable temperature is shown, which reaches up to 800 °C and remains almost constant from 12 noon to 3 pm, which is necessary to provide 600 °C minimum temperature for the reaction and start producing hydrogen and staying within the range until 4 pm. While in the cities of Morelia, Cuernavaca and Mexico City (CDMX) this profile becomes uneven due to periods of cloudiness, reaching a period of hydrogen production from 11 am to 2 pm.

In Fig. 8 the thermal behavior of the chemical reactor of 06/20/2018 of the city of Hermosillo (orange color) and the values of solar irradiation (red color) are observed. For these conditions the reactor quickly reached in less than 15 minutes the temperature of 600 °C and then a maximum temperature of 857 °C, with  $I_{max}$  of 1045 W/m<sup>2</sup> and without mediating any thermal control system, remaining within the range of operation and producing hydrogen for approximately 7 hours.



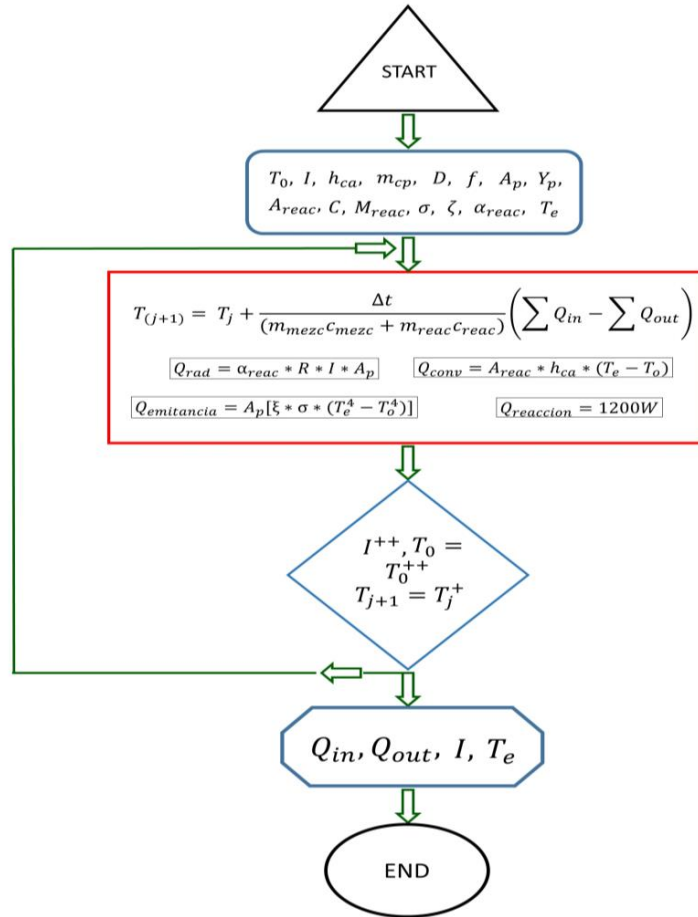


Fig. 6: Flow chart of the code used to simulate the reactor's energy balance.

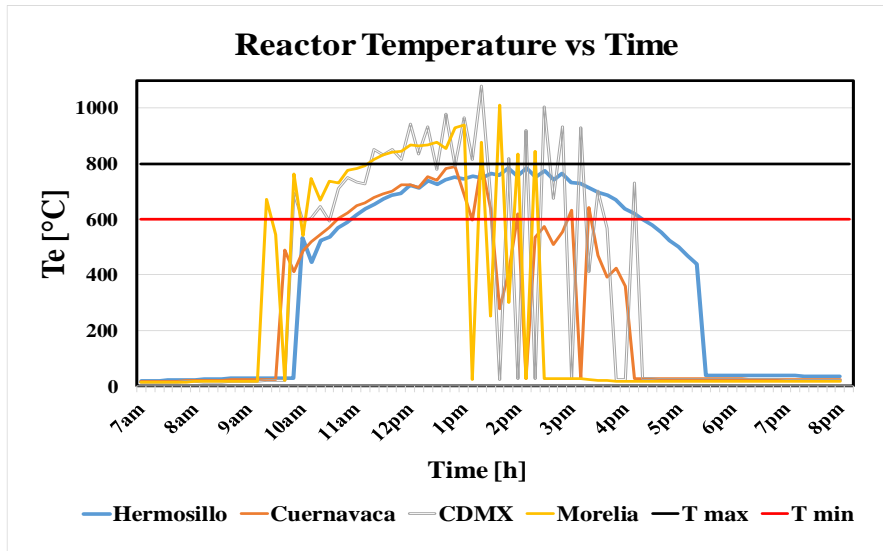


Fig. 7: Profile of reactor temperature evaluated in four Mexican cities.

Then it is easy to notice that it is in Hermosillo, Sonora, located in northwestern Mexico, in one of the areas with the highest solar irradiation in the world, it is where the system would best operate. But for economic reasons, for the moment, it is important that the system operates in Mexico City (CDMX).

For this reason, some simulations were carried out for different days, in order to find the most appropriate geometry, which allows the system to operate as many hours as possible, not only to reach the necessary operating temperature, but to maintain the longest time possible within the operating range to achieve the highest hydrogen production.

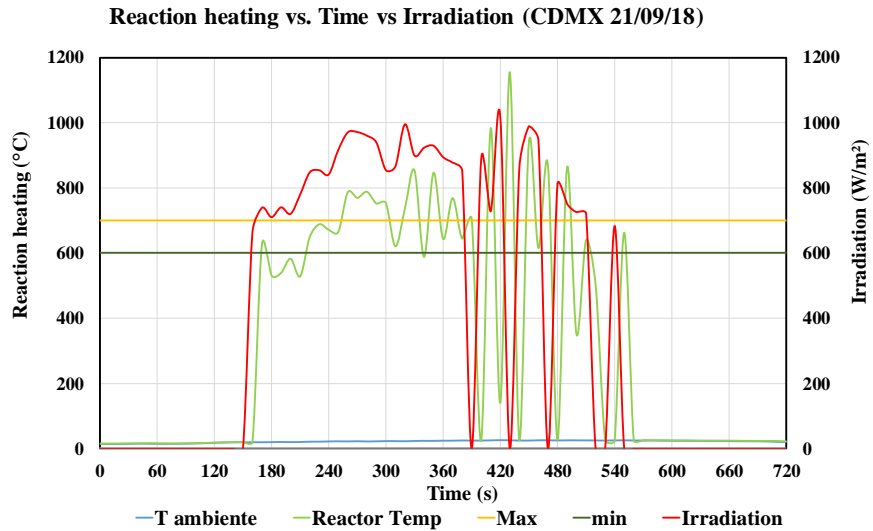


Fig. 8: Favorable day temperature profile Hermosillo Sonora.

Table 1 shows the main design parameters of the paraboloid, determined based on the thermal simulations performed, where the concentration ratio was particularly modified to achieve a higher operating temperature obtaining a longer operating time. Figure 9 presents the thermal behavior of the reactor according to the meteorological data of Mexico City (CDMX), corresponding to September 21, 2018.

Table 1. Simulation parameters for Mexico City (CDMX).

Dates	CDMX 21/9/18	CDMX 5/10/18	CDMX 24/10/18
Diameter (m)	2.3	2.4	2.4
Focus (m)	0.58	0.6	0.6
Concentration ratio (soles)	210	220	235
paraboloid area (m²)	5.9	5.3	5.6
High (Yp) (m)	0.56	0.58	0.60
Te Max (°C)	853	874	894
Te min (°C)	527	457	491
Irradiation (W/m²)	996	984	937
Useful time (h)	4	5	5.3

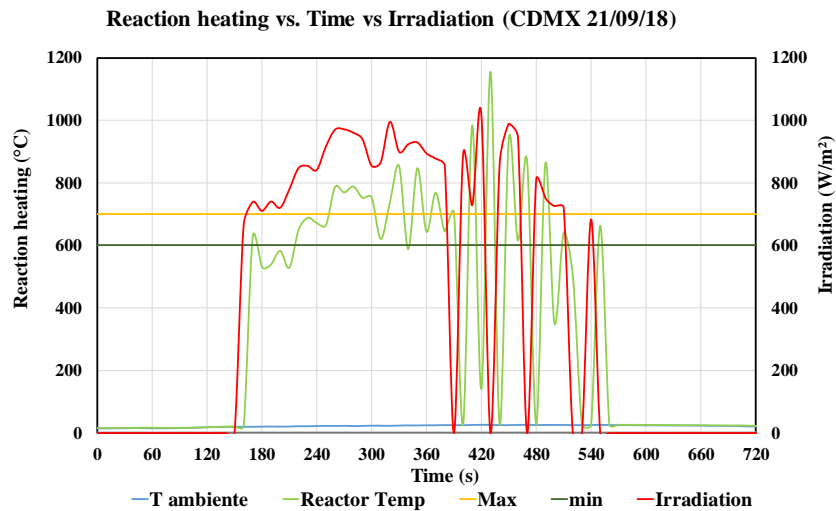


Fig. 9: Temperature profile of the thermochemical solar reactor operating in Mexico City, September 21, 2018 and shows the actual solar irradiation profile that was taken on the indicated date.

Thus, any of the configurations established in Table 1, can be used to design and build the paraboloid and experimentally test the solar thermal reactor to produce hydrogen in Mexico City.

### 5.1. Hydrogen Production

The results of the reactor performance in tests where the reactor was electrically heated for ethanol reforming at 550 °C are shown in Fig. 10 (a) and Fig. 10 (b), when the catalyst charge was 18 g. The catalyst was Ni-Co-Hydrotalcita and the ratio of water vapor to ethanol was four [13].

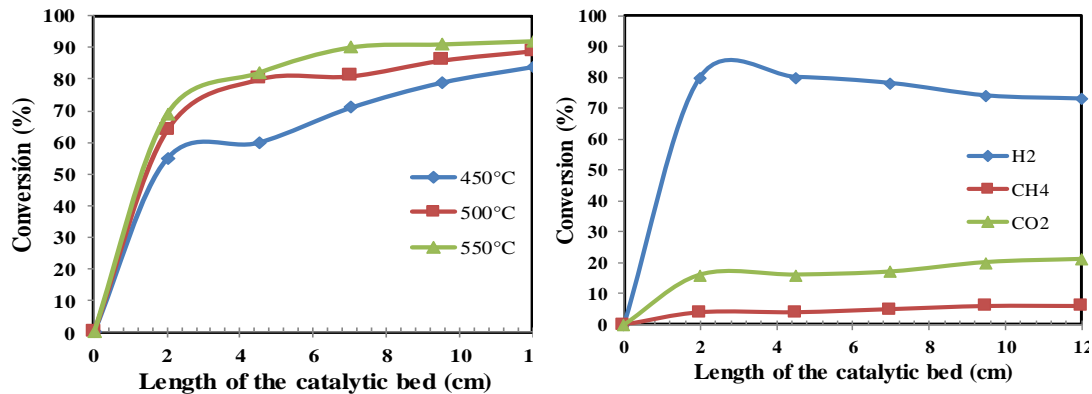


Fig. 10: (a) Conversion variation with respect to the length of the reactor. (b) Variation of the selectivity to H<sub>2</sub>, CH<sub>4</sub> and CO<sub>2</sub> as a function of the length of the reactor.

## 5. Conclusions

A mathematical model has been presented that allows the optical design of a parabolic solar concentrator to be coupled with a temporary energy balance, to calculate the temporal evolution of a thermochemical reactor for hydrogen production. The ratio of adequate solar concentration was obtained to reach the minimum temperature in the solar concentrator (reactor) to start the reaction and keep it within the temperature range of 600 to 700 °C. The simulation showed that the solar concentrator installed in Hermosillo Sonora, Mexico due to its higher average solar irradiation, can be generated with a smaller diameter and smaller area of the paraboloid, the temperature necessary for the production of hydrogen and maintain the reaction with the longest production time of hydrogen. It is demonstrated that it is feasible to carry out the ethanol vapor reforming reaction using conditions similar to those carried out when the reactor was heated with an electric oven. As noted, the reaction products were mainly H<sub>2</sub>, CH<sub>4</sub> and CO<sub>2</sub>.

## 6. Acknowledgments

The authors thank the CONACYT-SENER Energy Sustainability Fund for their financing for the project 249855.

## 7. References

- [1] P. F. Díez. Procesos termosolares en baja, media y alta temperatura, Cantabria: Servicio de Publicaciones de la Escuela T. Superior de Ingenieros de Caminos, Canales y Puertos, 1992.
- [2] R. Christoph, T. Sven, S. Rebecca. “Energía Solar Térmica de concentración: Perspectiva Mundial 2009. Greenpeace Internacional, SolarPACES y ESTELA, Junio 2009.
- [3] <https://www.energynews.es/proyecto-europeo-generar-hidrogeno-energia-solar/>. Consulted el 22 febrero de 2018.
- [4] <https://www.forbes.com.mx/paises-bajos-tendra-la-mayor-planta-de-hidrogeno-de-europa/> Consulted 23 febrero de 2018.
- [5] Kapdan, I.K., Kargi, F. (2006). Bio-hydrogen production from waste materials. *Enzym Micro Technology*, 38, 569-582.
- [6] IEA, Technology Roadmap – Concentrating Solar Power, 2010, <http://www.iea.org>.
- [7] H.I. Villafán-Vidales, C.A. Arancibia-Bulnes, D. Riveros-Rosas, H. Romero-Paredes and C.A. Estrada. An overview of the solar thermochemical processes for hydrogen and syngas production: Reactors, and facilities. *Renewable and Sustainable Energy Reviews* 75 (2017) 894–908.
- [8] A. Jaramillo and N. Daza, 2015, “Diseño, construcción y evaluación de una estufa solar para la cocción de alimentos”. Tesis de Ingeniero Físico. Universidad Tecnológica de Pereira, Colombia.
- [9] L.A. Andrade, M.A.S. Barrozo, L.G.M. Vieira. “A study on dynamic heating in solar dish concentrators.” *Renewable Energy*. Volume 87, Part 1, March 2016, 501-508.
- [10] Iván Rafael Martínez Cervantes, 2015, “Estudio de un reactor de lecho catalítico para la producción de hidrógeno a partir de bioetanol”. Tesis de Maestría en Ingeniería de Procesos. Universidad Autónoma Metropolitana Unidad Azcapotzalco.
- [11] Gregg DW, Taylor RW, Campbell JH, Taylor JR, Cotton A. Solar gasification of coal, activated carbon, coke and coal and biomass mixtures. *Sol Energy* 1980; 25:3 53–64.

- [12] F. Aguilar, 2018. Diseño y evaluación de un concentrador solar parabólico para la producción de hidrógeno. Tesis de Ing. Física. Universidad Autónoma Metropolitana, México.
- [13] Iván Rafael Martínez C., José Luis Contreras L, José Salmones, J.A. Colín L. y Carlos Tapia. Modelo de un Reactor de Lecho Catalítico para la Producción de Hidrógeno a partir de Bioetanol. 12 Congreso Interamericano de Computación Aplicada a la Ingeniería de Procesos, CAIP'2015, in Cartagena de Indias-Colombia, 14-17 Septiembre de 2015